New Substituted Copper Titanates with the $CaCu_3Ti_4O_{12}$ Structure: $Li[Cu_{3-x}Li_x][Ti_{3-x}M^V_{1+x}]O_{12}$ (M^V = Nb: $0.12 \leq x \leq 0.33$; M^V = Ta: $x = 0.33$)

PAULE MOURON AND JACQUES CHOISNET

Chimie Minérale, Université d'Orléans et C.R.P.H.T., CNRS BP 6759, F 45067 Orleans Cedex 2, France

New substituted copper titanates with the $CaCu_3Ti_4O_{12}$ perovskite-like structure were synthesized and characterized. Their formula is $Li|Cu_{3-x}Li_x|\,|Ti_{3-x}M^V_{1+x}|O_{12}$. There is a homogeneity range for M^V = Nb, $0.12 \leq x \leq 0.33$, and a unique composition for M^V = Ta, $x = 0.33$. The unit cell is cubic: $a \sim 2a_p$ (parameter of the ideal cubic cell) ~ 7.40 Å. The $CaCu_3Ti_4O_{12}$-type structure was confirmed from an X-ray powder structural determination. Lithium occupies both square planar sites where it replaces copper and icosahedral sites, with a probable delocalization. Crystal chemistry of the $AC_3B_4O_{12}$ structure is considered, taking into account the evolution of anion packing and the distortion of polyhedra. A diagrammatic representation is proposed so that precise information on the regularity of the $C_3B_4O_{12}$ network can be obtained. © 1987 Academic Press, Inc.

Introduction

Substituted copper(II) titanates with a high amount of copper show either the bixbyite-type structure of $(Fe,Mn)_2O_3$, as for the compounds $Cu_xTi_xFe_{2-2x}O_3$ (*1*), or a perovskite-like structure, as for $CaCu_3Ti_4O_{12}$ (*2*). In that case, a cooperative Jahn–Teller effect of copper(II) results in a distortion of the "ReO_3" framework, where three-fourths of cuboctahedral sites occupied by copper become square planar coordinated. The existence of this structure seems to be related to the unique composition $AC_3B_4O_{12}$, as emphasized by the numerous compounds prepared and characterized by Marezio *et al.*: [A = Na, Ca, Sr, Cd, Ln(III); B = Ti, Ge, Fe, Nb, Ta, Mn; C = Cu(II), Mn(III)] (*2, 5*). However, Cu(II)

and Mn(III) are not the only cations that lead to this structure type. Recently, lithium has been found in a square planar coordination in the bronzes $Li_{0.2}ReO_3$ and $Li_{0.36}WO_3$ (*6*), whose cubic structure with $a \simeq 2a_p$ (a_p: parameter of the ideal perovskite) is similar to that of $AC_3B_4O_{12}$.

Then, the presence of lithium in substituted copper titanates with a perovskite-like structure was considered. Owing to the good reactivity of $LiMO_3$ (M = Nb, Ta), CuO, and TiO_2 mixtures for preparing mixed oxides with the $LiNbO_3$-type structure (*7*), the synthesis of lithium-containing copper titanates was undertaken. The present results deal with the structural characterization of new mixed oxides with the formula $Li[Cu_{3-x}Li_x][Ti_{3-x}M^V_{1+x}]O_{12}$. From that result, crystal chemistry of the

TABLE I

Cubic Cell Parameters for
Li|Cu$_{3-x}$Li$_x$| |Ti$_{3-x}M^V_{1+x}$|O$_{12}$

M^V = Nb	$\begin{cases} x = 0.33 \\ x = 0.12 \end{cases}$	7.4314(3) Å 7.4212(6) Å
M^V = Ta	$x = 0.33$	7.425(1) Å

$AC_3B_4O_{12}$ structure is examined, taking into account the evolution of anion packing and the distortion of polyhedra.

Experimental

Compounds were prepared by heating stoichiometric mixtures of LiMO_3 (M = Nb, Ta), CuO, and TiO$_2$ in air in the ratio corresponding to the formula LiCu$_{3-x}$Li$_x$][Ti$_{3-x}M_{1+x}$]O$_{12}$, with $0 \le x \le 0.33$. Mixtures were first heated at 800°C, then at 950°C for Nb or 1000°C for Ta during 2 × 24 hr. Numerous grindings were made to ensure a complete reaction. For mixtures containing the highest amounts of Cu, the low reactivity requires several annealings at the final temperature.

Crystallographic characterization was made with a Guinier Nonius camera. Powder diffractograms were obtained from a Philips goniometer using CuKα radiation.

Results

New mixed oxides with the formula Li[Cu$_{3-x}$Li$_x$][Ti$_{3-x}M_{1+x}$]O$_{12}$ were obtained with a homogeneity range of $0.12 \le x \le 0.33$ for M = Nb and the unique composition $x = 0.33$ for M = Ta. Crystallographic analysis showed an excess of CuO and TiO$_2$ accompanying the limiting substituted compound for the compositions $0 \le x < 0.12$ (M = Nb) and $x < 0.33$ (M = Ta). Lower amounts of Cu ($x > 0.33$) led to the formation of small quantities of (Li, M)$_{1-y}$ (Cu, Ti)$_y$O$_3$ isotypic with LiNbO$_3$, which were recently characterized (7). It was not possible to isolate the composition $x = 0$ corresponding to the formula LiCu$_3$Ti$_3MO_{12}$. Thus, partial substitution of Cu for Li plays an important part in the existence of these oxides. Moreover, irrespective of the structure type, substituted copper(II) titanates seem to be stabilized for a (Cu, Ti)/O ratio close to 2/9 as in the bixbyite-type Cu$_x$Ti$_x$Fe$_{2-x}$O$_3$ oxides (1).

X-ray diffractograms of these titanates are similar to that of CaCu$_3$Ti$_4$O$_{12}$. They were indexed in a cubic cell with $a \sim 7.4$ Å $\sim 2a_p$. The values obtained after refinement (Table I) show a slight decrease when niobium is progressively replaced with titanium, in agreement with the respective size of ionic radii. Likewise, the tantalum compound has a somewhat smaller cell than the same niobium composition ($x = 0.33$). Moreover, the values observed here are very close to the value for NaCu$_3$(Ti$_3$Nb)O$_{12}$ (2): $a = 7.426$ Å.

A structural determination was made for the composition $x = 0.33$ (M = Nb), using the intensities of X-ray powder diffractograms. The only observed condition (hkl), $h + k + l = 2n$, led to the same space group $Im3$ as for CaCu$_3$Ti$_4$O$_{12}$ (2). According to the structural formula Li[Cu$_{2.67}$Li$_{0.33}$][Ti$_{2.67}$Nb$_{1.33}$]O$_{12}$, the atomic positions and their occupation are:

Li	2(a) 0 0 0	(Ti,Nb) 8c $\frac{1}{4}$ $\frac{1}{4}$ $\frac{1}{4}$
(Cu,Li)	6(b) 0 $\frac{1}{2}$ $\frac{1}{2}$	O 24(g) x y 0

The intensities of 19 observed reflections, i.e., 31 (hkl), were used for structure calculations (8). After refinement of the oxygen position and thermal parameters excluding the parameter of Li in 2(a), which is kept equal to 1 (Å)^2, the RI factor (RI = $\Sigma|I_o - I_c|/\Sigma I_o$) was decreased to 0.048. This result unambiguously confirms the validity of the CaCu$_3$Ti$_4$O$_{12}$-type structure for our compound. Atomic coordinates (Table II) of oxygen are close to the values obtained for the compounds which are isotypic with CaCu$_3$Ti$_4$O$_{12}$.

TABLE II

ATOMIC PARAMETERS FOR
$Li[Cu_{2.67}Li_{0.33}][Ti_{2.67}M_{1.33}]O_{12}$

	Li 2(a) or 24(g) $\tau = 1/12$	Cu, Li 6(b)	Ti, Nb 8(c)	O 24(g)
x	0	0.11(1)	0	$\frac{1}{4}$	0.310(1)
y	0	0.06(1)	$\frac{1}{4}$	$\frac{1}{4}$	0.180(1)
z	0	0	$\frac{1}{4}$	$\frac{1}{4}$	0
B (Å)^2	18.0	1.0(5)	1.0(1)	0.2(1)	1.1(3)

Note. τ: occupancy factor, Li 2(a): RI = 0.038, Li 24(g): RI = 0.036.

The presence of Li in 2(a) sites leads to 12 unusually long Li–O distances: 2.66 Å. Despite its weak X-ray scattering we attempted to obtain information on the location of Li. Including the thermal factor of Li in refinement calculations gives the lowest value of RI: 0.038 for $B(Li) = 18$ (Å)^2. This very large value probably shows a delocalization of Li which is no longer in 2(a). Therefore, we considered a possible location of Li in 24(g): x, y, 0 with an occupancy factor $\tau = 1/12$. RI is decreased to 0.036 for the following coordinates of Li: $x = 0.11$ (*1*), $y = 0.06$ (*1*), and a thermal factor now equal to 1 (Å)^2. In this configuration there is one Li–O distance close to 1.8 Å toward a vertex of the "O_{12}" icosahedral cavity. As a matter of fact, this result is only a partial answer to the problem of the location of Li, which will probably be solved by a neutron diffraction study.

These data show that the new oxides $Li[Cu_{3-x}Li_x][Ti_{3-x}M_x]O_{12}$ belong to the $AC_3B_4O_{12}$ family, with a perovskite-like structure. The C sites are square planar coordinated and the A sites are nearly icosahedral. The main feature concerning the Li-substituted compounds is the presence of Li both on A and C sites, Ti and Nb(Ta) being in octahedral coordination. Characteristic metal–oxygen distances and O–M–O angles for the composition $x = 0.33$ (Nb) are reported in Table III. These data are not as significant as those obtained from crystal structure determinations. However, the av-

erage distances (Ti, Nb)–O, 1.98 Å, and (Cu, Li)–O, 1.94 Å (square planar coordination), are close to the values calculated from ionic radii. The second set of (Cu, Li)–O distances, 2.77 Å, does not lead to a significant bonding. Angular distortions are weak, especially for the octahedra. Finally, the probable delocalization of Li in the A sites confirms the poor contribution of Li–O bonding to the stabilization of these oxides, as proved by the existence of lacunar □$C_3B_4O_{12}$ oxides such as $Cu_3Ta_2Ti_2O_{12}$ (*2*, *9*).

Discussion

"ReO_3" and "$C_3B_4O_{12}$" Frameworks: An Evolution of the Anion Packing

A description of the $AC_3B_4O_{12}$-type structure is obtained from the ideal perovskite model. Owing to the presence of Cu(II) or Mn(III), the "ReO_3" framework is distorted by a cooperative tilting of O–B–O

TABLE III

INTERATOMIC DISTANCES AND ANGLES FOR
$Li[Cu_{2.67}Li_{0.33}][Ti_{2.67}Nb_{1.33}]O_{12}$

Distance (Å)			Angle (°)		
Li–O	× 12	2.66(2)	O_B–Li–O_B	× 24	64.3(2)^a
			O_C–Li–O_C	× 6	60.2(3)^a
|Cu, Li|–O	× 4	1.94(1)	O_C–|Cu, Li|–O_C	× 2	86.9(4)^a
			O_C–|Cu, Li|–$O_{C'}$	× 2	93.1(4)^a
|Cu, Li|–O	× 4	2.77(2)			
|Cu, Li|–O	× 4	3.31(2)			
|Ti, Nb|–O	× 6	1.98(2)	O_B–|Ti, Nb|–O_B	× 6	91.4(4)^a
			O_B–|Ti, Nb|–$O_{B'}$	× 6	88.6(4)^a
O_B–O_B	× 4	2.84(2)^b	O_B–O_B–O_B	× 2	60.0^c
O_B–$O_{B'}$	× 4	2.77(2)^b	O_B–O_B–$O_{B'}$	× 4	59.2(2)^c
			O_B–$O_{B'}$–O_B	× 2	61.6(3)^c
O_C–O_C	× 1	2.67(2)^b	O_{BC}–O_{CB}–O_B	× 2	61.9(3)^c
			O_{CB}–O_B–O_{BC}	× 1	56.2(2)^c
O_C–$O_{C'}$	× 1	2.82(1)^b	$O_{BC'}$–O_{CB}–$O_{B'}$	× 2	59.4(2)^c
			O_{CB}–$O_{B'}$–$O_{BC'}$	× 1	61.3(3)^c

^{a} O_B, $O_{B'}$, oxygen belonging to the same octahedron and two different icosahedra; O_C, $O_{C'}$, oxygen belonging to the same square and two different icosahedra.
^{b} O_B–O_B, O_C–O_C: distances in the same icosahedron.
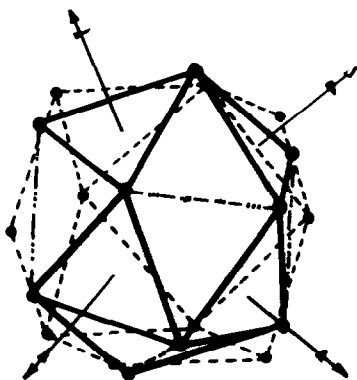^{c} Correspondence between distances and angles; for example, O_{BC}–O_{CB}–O_B.

FIG. 1. Relation between cuboctahedron and icosahedron after Wells (10).

chains with a tilting angle of (18–20°) for the members of the $AC_3B_4O_{12}$ family. Such a distortion allows the stabilization of a new framework, which differs from the "ReO₃" type by the participation of B in octahedral sites and C in square planar sites. The general formula of this framework is $C_3B_4O_{12}$.

As the cationic sublattice is identical to that of the ideal perovskite, anion packing should contribute significantly to the stabilization of the framework. Modifications in the anion packing result in an evolution of the competition between $M–O$ attraction forces and $M–M$ repulsion forces. Table III brings together the main O–O distances and O–O–O angles. The nearest neighbors of an oxygen anion are $5|4 + 1|$ from the same icosahedron and $5|2 + 2 + 1|$ from three different icosahedra, the coordination being an irregular 10-coordination. Thus two main evolutions concerning the anion packing can be pointed out:

—a decrease of the compacity, as compared to the close compact packing in ReO₃;

—a local increase of symmetry owing to the existence of icosahedra instead of cuboctahedra.

As emphasized by Wells (10), formation of regular icosahedra cannot lead to the most compact 3D framework. However,

the radiating structure obtained in that manner is the most symmetrical one. So, only considering a distortion of anion packing in the ReO₃ framework is a restricted description: it is a true reconstruction. Transformation of one-fourth of the cuboctahedra into icosahedra (Fig. 1) produces an increase of local order which balances the decrease of long-range order.

Connection between Icosahedra, Octahedra, and Squares: A Diagrammatic Representation

An idealized $C_3B_4O_{12}$ framework ensures a 3D connection between "O_{12}" icosahedra, BO_6 octahedra and CO_4 squares, as shown in Fig. 2. Icosahedra make a body-centered packing (Fig. 2a) where each "O_{12}" cluster is linked to its eight nearest neighbors through BO_6 octahedra and to its six second neighbors through CO_4 squares. Each octahedron shares two opposite faces with two icosahedra and each square shares two opposite edges with two icosahedra (Fig. 2b). As a result of the less compact anion packing, there is no space filling with polyhedra, unlike the "ReO₃" framework where the connection between cuboctahedra and octahedra gives a perfect space filling.

An actual $C_3B_4O_{12}$ framework is constructed from distorted polyhedra, owing to variable atomic positions of oxygen in $24(g)$: $x, y, 0$. Evolution of these distortions can be examined mathematically. Three independent relations between x and y account for the regularity of the polyhedra and the squares:

$$y^2 - x^2 + xy = 0,$$

regular icosahedra;   (I)

$$x + y - 2xy = \tfrac{3}{8},$$

regular octahedra;   (II)

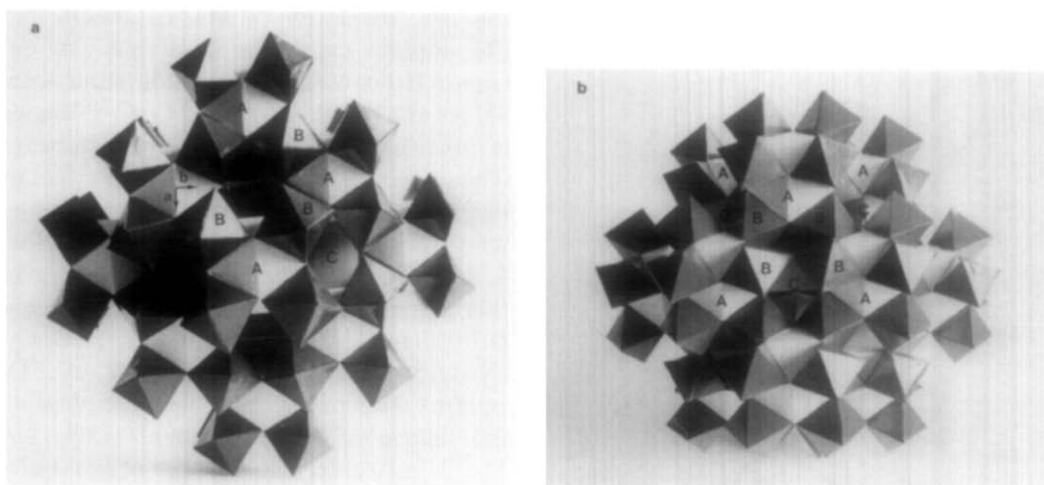$$x + y = \tfrac{1}{2},$$

regular squares.   (III)

Fig. 2. Idealized $C_3B_4O_{12}$ framework based on a 3D connection of tilted octahedra. (a) View along $\langle 001 \rangle$: an icosahedron (A) linked to four other ones, as the lower part of the body-centered packing. (b) View along $\langle 110 \rangle$: an octahedron (B) and a square (C) connected to two icosahedra (A).

These three relations cannot be simultaneously satisfied; therefore, two limiting cases must be considered:

(a) Regular icosahedra and octahedra: (I) and (II) are simultaneously satisfied. As a result, the anion packing is the most regular with a $|9 + 1|$ coordination.

(b) Regular icosahedra and squares: (I) and (III) are simultaneously satisfied, with a $|4 + 6|$ oxygen coordination of the anion packing.

Satisfying (II) and (III) leads to ideal perovskite structure, with cuboctahedra instead of icosahedra; values of x and y corresponding to the different cases are reported in Table IV.

The purpose of the diagrammatic representation drawn in Fig. 3 is to estimate geometrical characteristics of framework easily for the different members of the $AC_3B_4O_{12}$ family as well as for cubic lithium bronzes. Each compound in the diagram is represented by a particular point. Its position with respect to the (I), (II), or (III) curve gives information on the regularity of the corresponding polyhedra.

In the following, we try to identify the contribution of a particular element in the geometrical characteristics of the $AC_3B_4O_{12}$ structure. For the whole compounds, icosahedra are comparatively regular or show a small distortion coming from a tilting of

TABLE IV

MATHEMATICAL CONDITIONS FOR THE REGULARITY OF ICOSAHEDRA, OCTAHEDRA, AND SQUARES IN A $C_3B_4O_{12}$ NETWORK

(I)	Icosahedra	$y^2 - x^2 - xy = 0$	(I), (II) $x = 0.3009_5$, $y = 0.1860_0$
(II)	Octahedra	$x + y - 2xy = \frac{3}{8}$	(I), (III) $x = 0.3090_2$, $y = 0.1909_8$
(III)	Squares	$x + y = \frac{1}{2}$	(II), (III) $x = 0.250$, $y = 0.250$

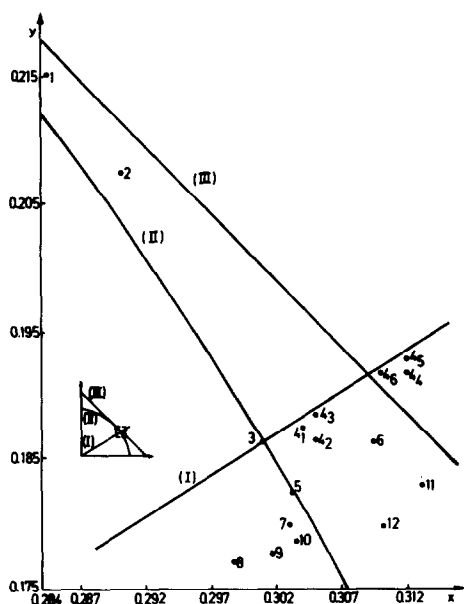Note. x and y are atomic coordinates for oxygen in $24(g)$: $x, y, 0$.

FIG. 3. Diagrammatic representation for the regularity of icosahedra (I), octahedra (II), and squares (III) in a $C_3B_4O_{12}$ framework. Compounds reported: No. 1: $Li_{0.2}ReO_3$ (6); No. 2: $Li_{0.36}WO_3$ (6); No. 3: $CaCu_3 Ge_4O_{12}$ (11); No. $4_{1 \rightarrow 6}$: $Cu_2Ta_4O_{12}$ (12); No. 5: $CaCu_3 Mn_4O_{12}$ (3); No. 6: $Cu_3Ti_2Ta_2O_{12}$ (9); No. 7: $Tb_{2/3}Cu_3 Ti_4O_{12}$ (2); No. 8: $ThCu_3Mn_4O_{12}$ (13); No. 9: $NdCu_3 Ti_3FeO_{12}$ (5); No. 10: $CaCu_3Ti_4O_{12}$ (2); No. 11: $NaMn_7O_{12}$ (4); No. 12: (Li, $Nb)_{1.33}(Cu, Ti)_{2.67}O_{12}$ (this work).

the B–O–B chains larger than 18°4, which corresponds to regular icosahedra; for our compound the tilting is 20°3 (No. 12 on the diagram). In $Li_{0.2}ReO_3$ and $Li_{0.36}WO_3$, tilting of the B–O–B chains is weak: 11°4 and 13°4. "O_{12}" polyhedra are "intermediate" between cuboctahedra and icosahedra. Thus, the regularity of icosahedra depends very little on the nature of the A element. On the other hand, it is related to the size of the B element in octahedral sites. In fact, the series of $CaCu_3B_4O_{12}$ oxides (B = Ti, Mn, Ge) (Nos. 10, 5, and 3) shows an increasing regularity of icosahedra as the size of B decreases.

Another interesting feature is clear from the diagram. Owing to the existence of ico-

sahedra, regularity of BO_6 octahedra and CO_4 squares cannot be simultaneously ensured. However, the deviation from ideal values (90°) for O–B–O and O–C–O angles is rather limited: it is within 3° for octahedra while it can reach 7° for squares. Perfect or nearly perfect octahedra are observed when the B element has a IV valency (Nos. 3, 5, 7, and 10), a decrease or an increase of this charge leading to a deviation from regularity as for $ThCu_3Mn_4O_{12}$ and $Cu_3Ti_2Ta_2O_{12}$ (Nos. 8 and 6). The geometry of CO_4 squares does not seem to be dependent on the nature of the C element (Cu^{II}, Li^I, Mn^{III}); conversely, the charge of the A element plays an important role; evolution of the most distorted squares, $ThCu_3Mn_4O_{12}$ (No. 8), to the most regular squares, $Cu_3Ti_2 Ta_2O_{12}$ and $NaMn_7O_{12}$ (Nos. 6 and 11), is related to a decreasing charge of the A element: +4 (Th), +3 (Nd, Tb), +2 (Ca), +1 (Li, Na), or 0 (vacancy). A decrease of electrostatic interactions between the A element and oxygen of an icosahedron appears and simultaneously a partial covalent character of C–O bonds is promoted. These facts agree quite well with an increasing regularity of CO_4 squares.

Two compounds of the $AC_3B_4O_{12}$ family show a specific behavior. The first, $CaCu_3 Ge_4O_{12}$, presents quasi-perfect icosahedra and octahedra, as pointed out by Ozaki et al. (11). The x and y values of oxygen atomic positions are extremely close to those simultaneously satisfying equations (I) and (II): 0.3012(5) and 0.1859(5) (Table IV). In the second, $Cu_2Ta_4O_{12}$, the A vacancy and the partial occupation of C sites by Cu bring about a weak orthorhombic distortion (12), leading to the existence of six different atomic positions for oxygen. Figure 3 shows an interesting feature: x and y values are distributed in two groups. The first group (Nos. 4_1, 4_2, 4_3) makes a major contribution to the regularity of octahedra while the second one (Nos. 4_4, 4_5, 4_6), especially, promotes the regularity of squares.

This analysis, directly made from the diagrammatic representation of Fig. 3, agrees with the conclusions of structural study on $Cu_2Ta_4O_{12}$ (12).

The major conclusions obtained from the diagrammatic representation are the following:

—The octahedra are the most regular for B^{IV} cations: an increase or a decrease of this charge leads to a distortion.

—The regularity of icosahedra slightly depends on the nature of the A element.

—The regularity of squares is closely related to the charge of A, nearly perfect squares being observed for the smallest charge.

Conclusion

New oxides with the formula $Li[Cu_{3-x}Li_x][Ti_{3-x}M_{1-x}]O_{12}$ (M = Nb, Ta; $x \leq$ 0.33) show all the characteristics of the $AC_3B_4O_{12}$-type structure, related to the perovskite type. Lithium plays an important part in stabilizing these compounds. It partially replaces copper in the square planar sites, as emphasized by the nonexistence of the composition $LiCu_3Ti_3MO_{12}$ (M = Nb, Ta), where only copper would be square planar coordinated. Lithium also occupies icosahedral A cavities with a probable delocalization. This will be defined in further studies.

The stability of an $AC_3B_4O_{12}$-type structure depends largely on anionic packing. Local formation of nearly regular icosahedra equilibrates the increase of repulsion forces between B cations which is created by the tilting of B–O–B chains. This is confirmed by the existence of several mixed oxides where distortions of octahedral framework lead to formation of "O_{12}" icosahedra; that is the case for the oxides $ACu_3M_7O_{21}$ (14), which are intergrowths of "$Cu_3M_4O_{12}$"-type blocks and "AM_3O_9" hexagonal bronze blocks, and equally for the hexagonal bronze $K_{0.9}Mo_6O_{17}$ (15), where "ReO_3"-type blocks are connected by "KO_{12}" icosahedra. A diagrammatic representation based upon mathematical conditions for the regularity of polyhedra produces rapid information on their respective distortions.

Work is in progress to define the role of the copper–lithium pair on the stabilization of compounds with an $AC_3B_4O_{12}$ structure.

References

1. P. MOURON, P. ODIER, AND J. CHOISNET, J. Solid State Chem. 60, 87 (1985).
2. B. BOCHU, M. N. DESCHIZEAUX, J. C. JOUBERT, A. COLLOMB, J. CHENAVAS, AND M. MAREZIO, J. Solid State Chem. 29, 291 (1979).
3. J. CHENAVAS, J. C. JOUBERT, M. MAREZIO, AND B. BOCHU, J. Solid State Chem. 14, 25 (1975).
4. M. MAREZIO, P. D. DERNIER, J. CHENAVAS, AND J. C. JOUBERT, J. Solid State Chem. 6, 16 (1973).
5. C. MEYER, Y. GROS, B. BOCHU, A. COLLOMB, J. CHENAVAS, J. C. JOUBERT, AND M. MAREZIO, Phys. Status Solidi A 48, 581 (1978).
6. R. J. CAVA, A. SANTORO, D. W. MURPHY, S. M. ZAHURAK, AND R. S. ROTH, J. Solid State Chem. 50, 121 (1983).
7. P. MOURON AND J. CHOISNET, J. Phys., Colloq. C1, 47, 491 (1986).
8. C. C. PHAM, J. CHOISNET, AND B. RAVEAU, Bull. Acad. R. Belg. Cl. Sci. 61, 473 (1975).
9. VON V. PROPACH, Z. Anorg. Allg. Chem. 435, 161 (1977).
10. A. F. WELLS, "Structural Inorganic Chemistry," Univ. Press (Clarendon), London/New York (1984).
11. Y. OZAKI, M. GHEDIRA, J. CHENAVAS, J. C. JOUBERT, AND M. MAREZIO, Acta Crystallogr. Sect. B 33, 3615 (1977).
12. H. VINCENT, B. BOCHU, J. J. AUBERT, J. C. JOUBERT, AND M. MAREZIO, J. Solid State Chem. 24, 245 (1978).
13. M. N. DESCHIZEAUX, J. C. JOUBERT, A. VEGAS, A. COLLOMB, J. CHENAVAS, AND M. MAREZIO, J. Solid State Chem. 19, 45 (1976).
14. A. BENMOUSSA, D. GROULT, F. STUDER, AND B. RAVEAU, J. Solid State Chem. 41, 221 (1982).
15. H. VINCENT, M. GHEDIRA, J. MARCUS, J. MERCIER, AND C. SCHLENKER, J. Solid State Chem. 47, 113 (1983).